Chemical Science

ROYAL SOCIETY OF CHEMISTRY

EDGE ARTICLE

View Article Online
View Journal | View Issue

Cite this: *Chem. Sci.*, 2025, **16**, 19981

All publication charges for this article have been paid for by the Royal Society of Chemistry

DNA aggregation and resolubilization in the presence of polyamines probed at the single molecule level using nanopores

Yuhua Cai,[a] Benjamin Cressiot,[b] Sébastien Balme,[c] Eric Raspaud,[d] Laurent Bacri *[a] and Juan Pelta *[a]

The compaction and decompaction of double-stranded DNA play a crucial role in regulating gene expression. We use solid-state nanopores to study, at the single-molecule level, the translocation of DNA chains in relation to the macroscopic phase transition induced by polyamines. To prevent nonspecific interactions between the nanopore surface and DNA, nanopores were passivated, and experiments were performed in high salt conditions. We first determine the translocation dynamics of DNA. The event frequency varies exponentially with the applied voltage and linearly with the polyelectrolyte concentration. The translocation time decreases exponentially with applied voltage. Addition of polyamine to a DNA solution leads to DNA aggregation and subsequent phase separation; a macroscopic DNA-rich and dense phase coexists with a poor-DNA (diluted) phase. We pipetted part of the diluted phase and studied chain translocation. We observe a progressively decreasing event frequency of DNA in the solution at the nanopore entry as a function of polyamine concentration, approaching zero Hertz. At this point, no DNA remained in the poor phase, and all the DNA was found in the precipitated rich phase. If we increase the polyamine concentration even further, the event frequency increases progressively until it reaches a plateau value due to the solubilization of DNA aggregates. At high salt concentrations in NaCl, we observe that the event frequency of DNA in solution remains constant as a function of polyamine concentrations. We compare DNA phase transitions using nanopore and UV bulk experiments, and we find the same charge-to-molar ratio for DNA precipitation and solubilization. We interpret these results through polyelectrolyte behavior.

Received 15th July 2025
Accepted 25th September 2025

DOI: 10.1039/d5sc05267j

rsc.li/chemical-science

Introduction

DNA compaction and decompaction are essential for numerous cellular processes, including gene regulation, chromatin organization, and viral genome packaging.[1–3] Genome organization is also implicated in human disease, and chromatin organization plays a crucial role in the efficiency of DNA repair and the aging process.[4] It is really important to study and understand the compaction and decompaction of DNA. Polyamines are polycationic molecules that contain amino groups (2 to 4), and these aliphatic amines are present in all eukaryotic and prokaryotic cells.[5] Polyamines can interact with negatively charged biological molecules, including DNA, RNA, and phospholipids. These polycations are involved in numerous physiological processes and biological functions, including cell division and proliferation, cell–cell communication, cell survival, DNA and protein synthesis, apoptosis, oxidative stress, and angiogenesis. Polyamines are also involved in human diseases such as cancer.[6,7] DNA phase transitions are strongly influenced by natural multivalent cations, such as spermidine (3^+) and spermine (4^+),[8] or by basic proteins, including histone H1 or protamines,[9] which can induce DNA condensation.[10] These mechanisms are explained by the molecular theory of polyelectrolytes in solution with applications to the electrostatic properties of DNA. In the presence of these electrically positively charged molecules, collapse or aggregation of DNA occurs as a function of the polyelectrolyte chain length and concentration.[11] Different techniques, such as UV absorbance, electronic microscopy, and laser light scattering, have been widely used to monitor DNA aggregation or collapse in the presence of polyamines or other multivalent cations.[12–16] Depending on the concentration, a diluted DNA phase coexists with a rich and dense, usually liquid-crystalline phase.[8] Here, we are interested in the diluted chains and wonder if these chains can be further counted and analyzed individually. It is possible to probe DNA

[a]*Université Paris-Saclay, Univ Evry, CY Cergy Paris Université, CNRS, LAMBE, 91025 Evry-Courcouronnes, France. E-mail: laurent.bacri@univ-evry.fr; juan.pelta@univ-evry.fr*

[b]*Université Paris-Saclay, Univ Evry, CY Cergy Paris Université, CNRS, LAMBE, F-95000 Cergy, France*

[c]*Institut Européen des Membranes, UMR5635 UM ENSM CNRS, Place Eugène Bataillon, 34095 Montpellier Cedex 5, France*

[d]*Université Paris-Saclay, CNRS, Laboratoire de Physique des Solides, 91405 Orsay, France*

phase separation, aggregation, and solubilization using electrical measurements. Will the threshold polycation concentrations, spermidine and spermine, for DNA phase separation be the same or different for single-molecule and volume experiments?

To the best of our knowledge, the translocation and counting of DNA chains at the single molecular level, using a solid-state nanopore, has never been studied in relation to the phase transition of DNA. In this technique, two compartments with an electrolyte solution are separated by a nanohole. A constant potential difference applied between the two electrodes leads to an ionic current due to the flow of ions through the nanopore. Under the driving force, a molecule passing through the nanopore or interacting with it partially blocks ion transport, leading to a decrease in ionic current. The resulting ionic current blockades provide information on the size, conformation, chemical modifications, sequence, and enantiomers of the species.[17–21]

Previously, nanopore works have shown the great potential of this single-molecular technique to probe protein phase transitions, from native to unfolded states. Unfolding curves of proteins have been obtained using chemical denaturing agents,[22,23] temperature,[24] under applied voltage,[25,26] or with the aid of a molecular motor.[27] The unfolding transition does not depend on the nanopore structure.[28] Still, the denaturation transition is affected, respectively, by the stability or instability of the protein, whether wild type or mutant. The melting transition remains the same at both the bulk and single molecular levels.[24] A glassy behavior is experimentally demonstrated using a chaotropic agent during the unfolding process.[23] Notably, chaotropic agents have been shown experimentally not only to mediate the glassy behavior during protein unfolding but also to play a key role in nanopore stoichiometry, while stabilized nanopores enable precise discrimination of biopolymers at the single-molecule level.[29] Beyond protein unfolding, nanopores have also been employed to probe protein self-assembly and aggregation processes, such as those mediated by heparin reagents or chiral residue introduction,[30] further expanding the application of nanopore technology in studying biomolecular phase transitions. Some previous papers show the ability of nanopores to probe amyloid detection.[31–33] Another example of polymer transition as a function of temperature has been described. An increase in temperature leads to an extension of the size discrimination range of a polymer (polyethylene glycol, PEG) by a protein channel. This increase in temperature leads to the collapse of this long polymer chain into a globule, after which the molecule explores the confined medium and restores resolution in terms of size discrimination.[34]

Solid-state nanopores provide a platform for investigating DNA transport and interactions as a function of applied voltage,[35] salt gradient,[36] or chain length.[37] Other studies characterize different configurations with or without a hairpin structure,[38,39] including several topological states, such as knots[40] (linear, circular, relaxed, or supercoiled forms[41]). Single nucleotides[42] and amino acids[43] have also been identified.

Understanding DNA phase transition at the single-molecular level remains challenging. Is it possible to count each chain, with a nanopore approach, in relation to the transition? As a prospect, is it possible to detect its DNA conformational change dynamics? How fast should the dynamics of a collapsing DNA be due to the polyamine-induced attractive interactions? In the first attempt, we study here the translocation of chains in 1.2 M NaCl, where electrostatic interactions (both attractive and repulsive) are strongly attenuated. At 1.2 M NaCl, the high ionic conductivity of the solution stabilizes the baseline ionic current through the nanopores, reducing fluctuations (noise) and enhancing the signal-to-noise ratio. We utilize passivated solid-state nanopores to prevent interaction between the DNA and the nanopore surface. We compare the fraction of diluted chains as detected by a single molecular approach and by conventional UV bulk experiments at the end.

Results and discussion

Dynamics of DNA through a solid-state nanopore

Solid-state nanopores are fabricated using a controlled breakdown approach[38,44] and characterized by current–voltage (I–V) curves (Fig. S1). To prevent interaction between DNA and the nanopore surface, we functionalized the surface with L-Dopa[45] (Fig. S1). We observe a linear dependency of the current as a function of voltage, both before and after functionalization, exhibiting ohmic behavior (Fig. S1c). The ionic conductance is due to ion transport through the nanopore, a phenomenon previously observed with solid-state nanopores.[46] The I–V curve slope of the linear fit represents the ionic conductance of the nanopore (G) and decreases with L-Dopa. We obtain, respectively, $G_{\text{Raw}} = 12.1 \pm 0.4$ nS without functionalization and $G_{\text{L-Dopa}} = 6.3 \pm 0.3$ nS with functionalization. We deduce a reduction in nanopore diameter from 4.4 ± 0.4 nm to 3.5 ± 0.2 nm, which is higher than the double helix diameter (2 nm). The number of DNA spikes is lower without functionalization (Fig. S2).

We study the dynamics of DNA as a function of polyelectrolyte concentration and applied voltage. We work at a fixed NaCl concentration of 1.2 M. Current data values are recorded over time at a sampling time of 5 microseconds, as illustrated in Fig. 1B; spikes are observed and increase with DNA concentration. In our experimental conditions, the mean dwell time (Fig. S3) is independent of the DNA concentration (Fig. 1c), yielding a value of $\langle t \rangle = 143 \pm 10$ μs. The event frequency is defined as the number of events per second detected by the nanopore (Hz). As the characteristic time τ is similar to the period of a periodic signal, it is relevant to consider that the inverse of this time is a frequency in Hz (s^{-1}).

We find a linear behaviour of event frequency (Fig. S4) as a function of DNA concentration (Fig. 1d). The DNA does not strongly interact with the nanopore. We observe a threefold increase in the slope of the linear fit with nanopore functionalization compared to without functionalization (Fig. S2). This indicates that the entry of DNA molecules into the nanopore is facilitated by functionalization. The number of blockade events and the current through the empty nanopore increase with the applied voltage (Fig. 1e). The mean dwell time (Fig. S5) decreases exponentially with the electrical force, indicating that the DNA molecule is well transported through the nanopore

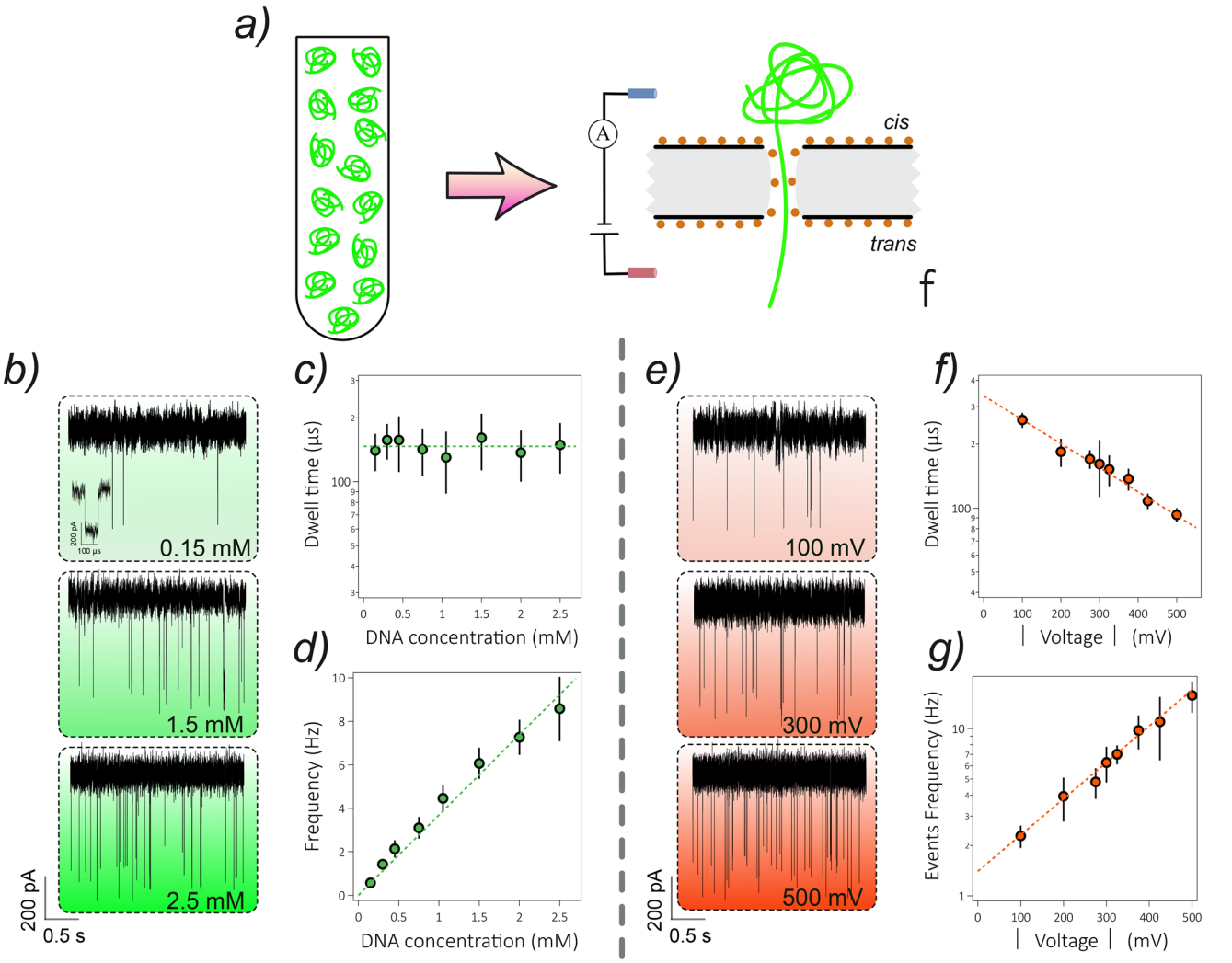

Fig. 1 DNA translocation dynamics through L-Dopa-modified solid-state nanopores under varying concentrations and voltages. (a) Dynamics of DNA through solid-state nanopores with L-Dopa. (b) Part of current traces as a function of DNA concentrations (0.15–2.5 mM). (c) Dwell time *versus* DNA concentrations. (d) Event frequency evolution as a function of DNA concentration. (e) Part of the current traces of DNA at different voltages. Event frequency (f) or dwell time (g) as a function of applied voltage. The fits correspond to $f = f_0 \cdot \exp(V/V_0)$, where $f_0 = 1.4$ Hz $\pm$ 0.2 Hz et $V_0 = 200$ mV and $f = A \cdot \exp(-V/V_c)$ where $A = 338$ μs and $V_c = 384.6$ mV. Experimental conditions are: 1.2 M NaCl, 10 mM Tris-HCl, pH 7.6, 1 mM EDTA, and DNA of 1 kbp. The error bars represent data collected from at least 3 independent samples prepared and by the nanopore device. And for each experimental condition, the error is derived from the standard deviation of the measurements.

(Fig. 1f). We also observe that event frequency (Fig. S6) increases exponentially with voltage (Fig. 1g). The DNA entry into a confined medium under an electrical force can be described by an activated process associated with an energy barrier.[47–49] The exponential function, $f = f_0 \cdot \exp(V/V_0)$, where $f_0 = p \cdot \nu \cdot \exp(-U/k_BT)$ is the frequency in the absence of applied voltage, p is a probability factor, ν a frequency factor, U is the activation energy, k_BT is the thermal agitation, and V is the applied voltage. We find $f_0 = 1.4$ Hz $\pm$ 0.2 Hz and estimate ν at 3817 Hz. The calculated energy barrier U is equal to 8.0 $\pm$ 1.1 k_BT. The diameter of the double-strand DNA of one 1 kbp, with a persistence length of 50 nm, is larger by a factor of 30 compared to the nanopore diameter. The main contribution of the energy barrier is due to chain confinement within the confined medium. This process of chain entry is therefore entropically unfavorable because it restricts the number of conformations of a DNA molecule that can be found during translocation.[50] A high energy barrier of 12 k_BT was previously deduced from an Arrhenius plot[35] when DNA translocated through a pore of similar diameter, and for a surface-oxidized SiN pore (*i.e.*, negatively charged) then passivated with a zwitterion (DOPA). Through larger conical quartz nanopores, 15 nm in diameter, the energy decreased to 4 k_BT at a high salt concentration (4 M LiCl),[51] an ionic condition that also strongly reduced the effective diameter of the DNA double helix itself.

DNA aggregation and resolubilization induced by polyamines and the effect of salts

We studied DNA stability in the presence of spermidine (3^+) or spermine (4^+) using solid-state nanopores at both low and high

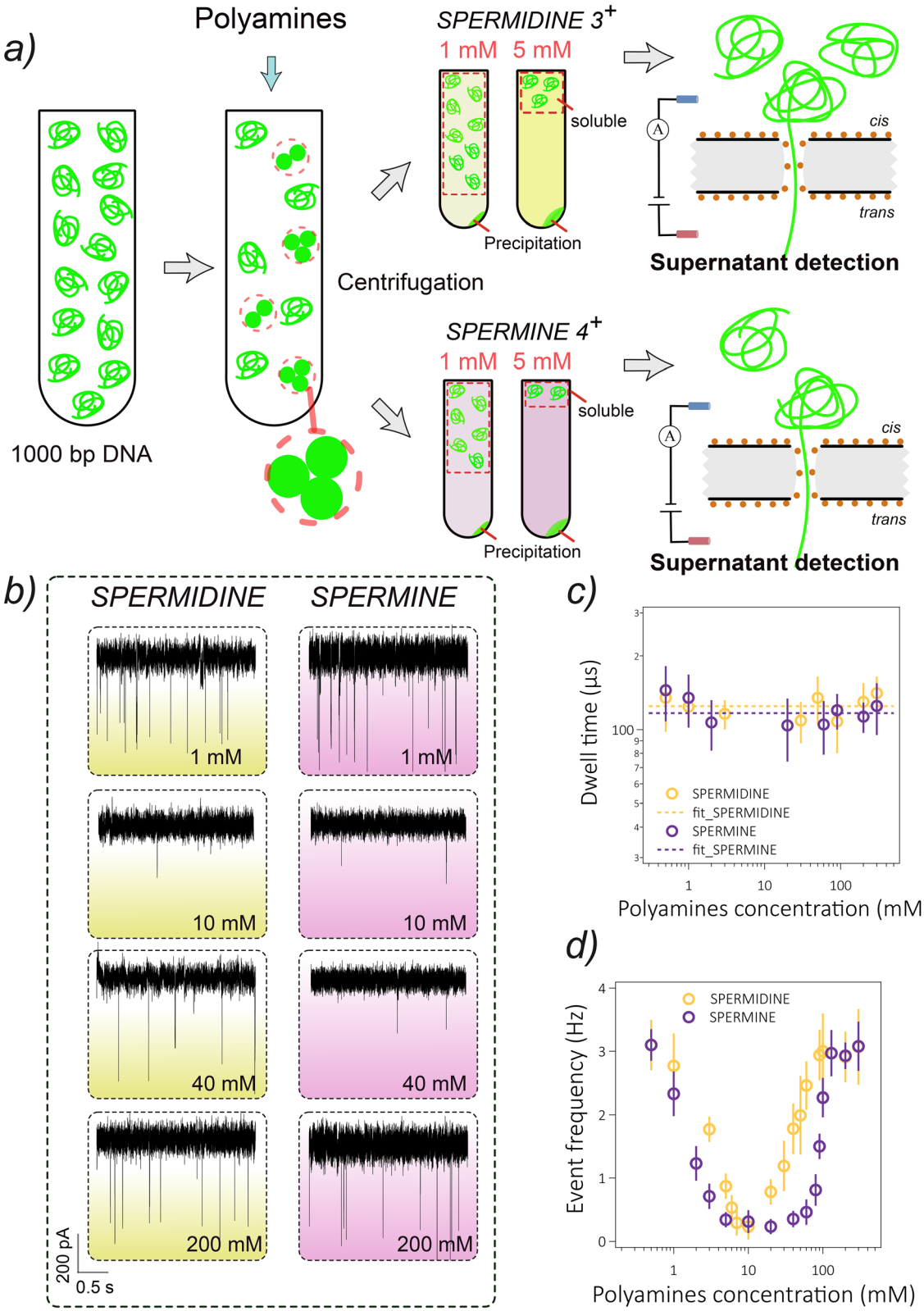

Fig. 2 Effect of polyamine concentration on DNA stability. (a) DNA stability as a function of polyamine concentrations (between 0.5 mM and 300 mM). After centrifugation, the supernatant is diluted in 1.2 M NaCl and transferred into the nanopore detection system. (b) Evolution of the part of current traces as a function of different polyamine concentrations used. (c) The dwell time of DNA as a function of spermidine or spermine concentrations. (d) Event frequency evolution as a function of spermidine or spermine concentrations. The applied voltage is fixed at −300 mV. Experimental conditions are: 1.2 M NaCl, prepared in a TE buffer consisting of 10 mM Tris–HCl, pH 7.6, and 1 mM EDTA. The error bars represent data collected from at least 3 independent samples prepared and by the nanopore device. And for each experimental condition, the error is derived from the standard deviation of the measurements.

NaCl concentrations. In our experiments, the 1 kbp DNA concentration is fixed at 0.75 mM, and the concentration of polyamines is varied between 0.5 mM and 300 mM. The NaCl concentration is initially kept constant at 25 mM. At this NaCl concentration, addition of a low concentration of polyamine to a DNA solution results in the formation of large and dense DNA aggregates. To precisely probe this DNA phase transition, the sample is centrifuged immediately after polyamine addition, and only the supernatant is pipetted and brought into contact with nanopores in 1.2 M NaCl (Fig. 2a). The large amount of Na^+ cations is expected to compete with polyamine counterions initially condensed onto DNA. This competition leads to the presence of Na^+ counterions, which suppress attractive electrostatic interactions. As a consequence, pipetted chains in contact with nanopores are expected to behave mostly like DNA chains without polyamines.

At low concentrations of spermidine or spermine, we observe some spikes in the current traces, which are attributed to the presence of DNA in the solution. The increase in polycation concentration leads to a decrease in spikes. If we increase the polycation concentration even further, the number of spikes increases (Fig. 2a). We have plotted the dwell time of current blockade (Fig. S7 and S8) as a function of polyamine concentration (Fig. 3c). We show that this mean dwell time is independent of spermine (3^+) or spermidine (4^+) concentration used. We find, respectively, $\langle t \rangle = 125 \pm 8$ μs and $\langle t \rangle = 117 \pm 6$ μs for the trivalent and tetravalent polycations. These events correspond to the same DNA conformation detected by the nanopore. These values are slightly lower than $\langle t \rangle = 143 \pm 10$ μs, the dwell time measured in the absence of polyamines. We suspect that this is due to the effective charge modification of the DNA. Condensation of z-valent counterions onto DNA is

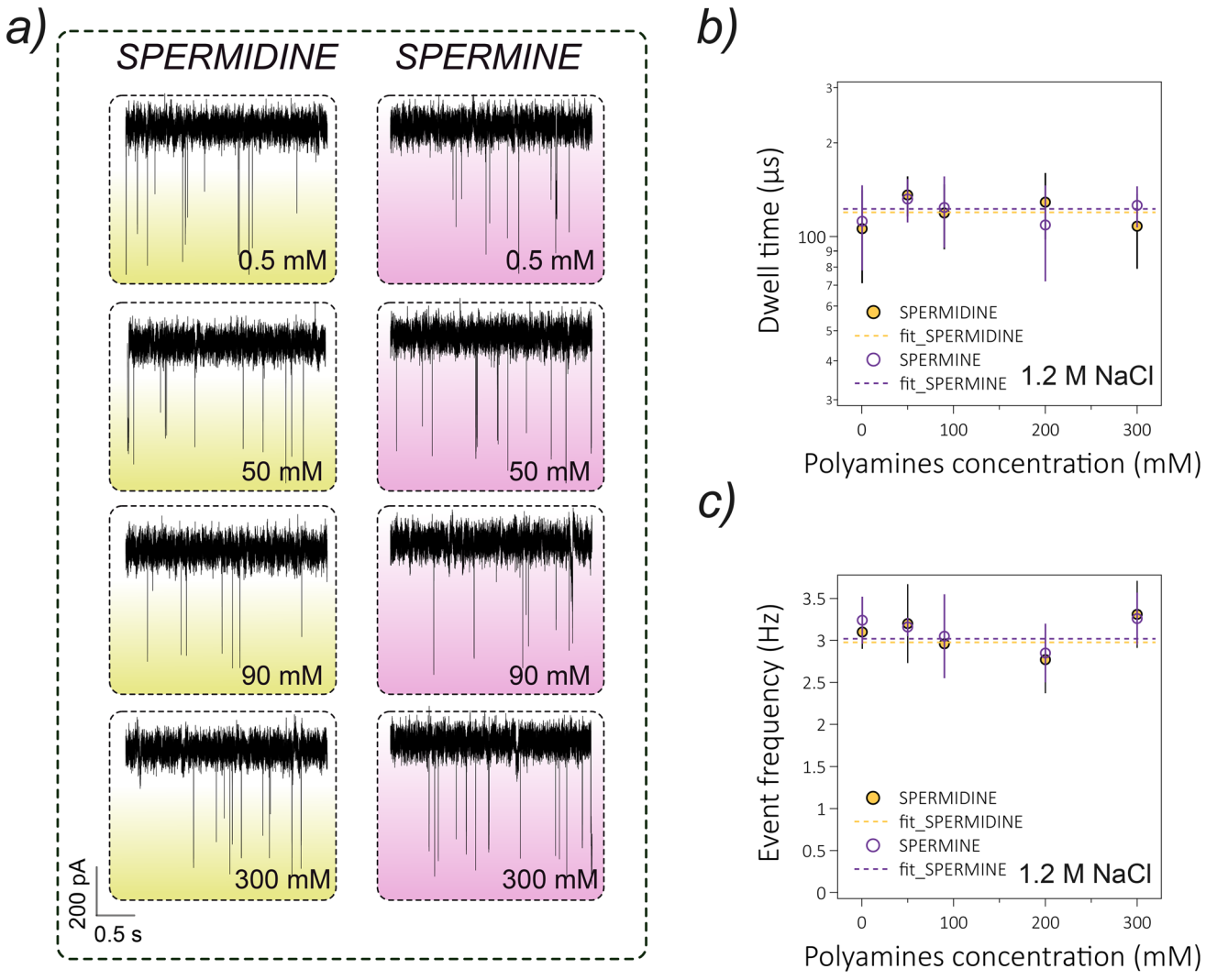

Fig. 3 Suppression of DNA precipitation in high salt conditions. (a) Part of the current trace of 0.75 mM DNA as a function of polyamine concentration at high salt concentration. (b) Event frequency of DNA at different spermidine and spermine concentrations (0.5–300 mM) in 1.2 M NaCl, 10 mM Tris HCl, pH 7.6, 1 mM EDTA. (c) The dwell time of DNA at different spermidine and spermine concentrations (0.5–300 mM) in 1.2 M NaCl, 10 mM Tris HCl, pH 7.6, 1 mM EDTA. The applied voltage is fixed at −300 mV. The error bars represent data collected from at least 3 independent samples prepared and by the nanopore device. And for each experimental condition, the error is derived from the standard deviation of the measurements.

known to reduce its effective charge: from 76% ($z = 1$, sodium cations) to 92% ($z = 3$, spermidine) and 94% ($z = 4$, spermine) according to Manning's model.[10] In this model, the fraction of "condensed" counterions along the polyelectrolyte is given by $f_c = 1 - 1/|\xi z_i z_n|$, where ξ represents the linear charge density of the polyelectrolyte equal to 4.2 for double-strand DNA, z_i represents the ion valence and z_n the polyelectrolyte valence. Here, pre-dilution in 1.2 M NaCl before translocation experiments is expected, on the one hand, to release the initial z-valent counterions from the DNA and increase the effective DNA charge, and, on the other hand, to strongly reduce any electrostatic effects. Therefore, we suspect that the small difference measured in dwell time results from the presence of residual polyamine counterions.

In Fig. 2a, we plot the event frequency as a function of polyamine concentration. Between 0.5 mM and 10 mM of spermidine or spermine, the event frequency (Fig. S9 and S10) decreases from 3.1 ± 0.2 Hz to 0.2 ± 0.1 Hz, and then the DNA is precipitated. Higher concentrations of spermine or spermidine progressively increase the event frequency, and the amount of DNA precipitated decreases. At a polyamine concentration of 90 mM, the event frequency reaches a plateau value of around 3 Hz. In the same experimental conditions without polyamine addition, the frequency is also around 3 Hz, indicating that DNA aggregation is completely suppressed.

In our experimental conditions, we demonstrate the resolubilization of DNA (the re-entrant phase transition) in the presence of polyamines. These results on DNA phase separation by polyamines are in good agreement with bulk experiments performed previously using a short DNA double strand of 146 bp in length.[14–16]

To investigate the effect of ionic strength on DNA stability and aggregation, we conducted a new set of DNA-polyamines mixing at a high salt concentration, with NaCl equal to 1.2 M. At this salt concentration, the Debye length is equal to 0.88 nm, and in the same order as the Bjerrum length, 0.71 nm, then the electrostatic interactions in solution are expected to be screened.

For different concentrations of polyamines used, we observe, from the current traces, that the number of spikes is the same (Fig. 3a), indicating that the DNA remains in solution. We verified that the dwell time (Fig. S11 and S12) of the DNA molecule is independent of the polycation concentration (Fig. 3b). We find respectively $\langle t \rangle$ 123 ± 5 μs and $\langle t \rangle$ =120 ± 6 μs for the spermidine and the spermine. The polyamine concentration does not affect the frequency of events (Fig. S13 and S14), as we find respective frequencies of 3.0 ± 0.3 Hz and 3.0 ± 0.4 Hz for spermidine and spermine (Fig. 3c) and 3.1 Hz for DNA alone. These results show that DNA precipitation is completely prevented, regardless of the polyamine concentration used (up to 300 mM). The phenomenon of DNA precipitation suppression, as observed in bulk experiments, has been previously reported, starting with 100% short DNA precipitation (with 25 mM spermidine), which leads to a sigmoidal curve of DNA in solution (0%) as a function of NaCl concentration (mM).[14]

The next step is to compare nanopore experiments to classical bulk experiments to study the DNA phase transition (Fig. 4). After the addition of polyamine, the amount of DNA remaining in the supernatant (diluted fraction) or the percentage of DNA in solution was determined by measuring the absorbance at 260 nm. To compare all the results, we have normalized the maximum event frequency to 100% of the DNA in solution for spermidine (Fig. 4a) and spermine (Fig. 4b). We have obtained the same behavior for the evolution of DNA in solution as a function of polycation concentration in both single-molecule and bulk experiments. The experimental data are superimposed on a single curve for each type of polycation. We show a precipitation phase of DNA solution at low polyamine concentration, followed by a progressive resolubilization

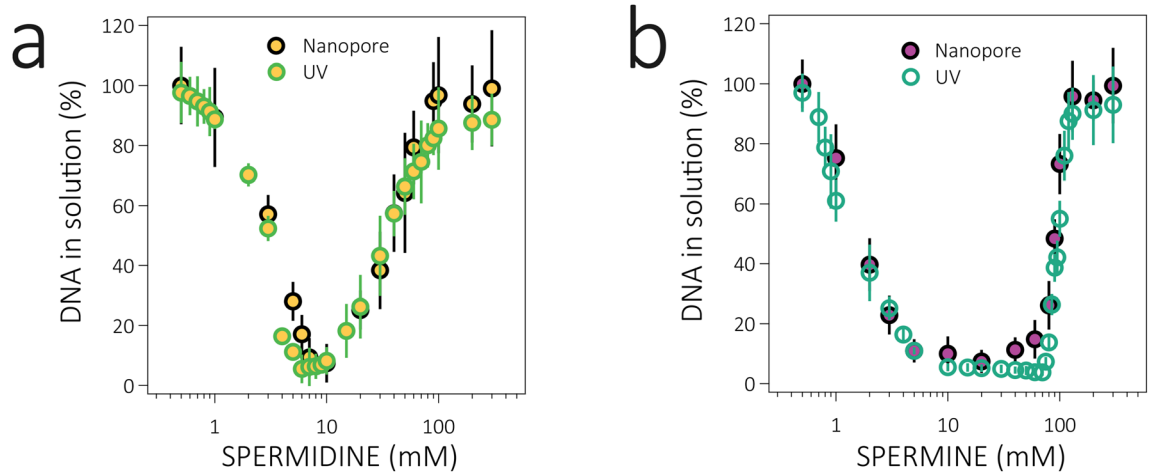

Fig. 4 (a) Concentration of spermidine *versus* normalized number of events (%) and DNA in solution (%). (b) Concentration of spermine *versus* normalized number of events (%) and DNA in solution (%). The UV absorption at 260 nm. The voltage for nanopore detection is −300 mV. Buffer: 1.2 M NaCl, 10 mM Tris HCl, pH 7.6, 1 mM EDTA; DNA: 0.75 mM. The error bars represent data collected from at least 3 independent samples prepared and by the nanopore device. And for each experimental condition, the error is derived from the standard deviation of the measurements.

of DNA aggregates at higher polyamine concentration. We observe a quantitative difference in the precipitation and resolubilization phase. The amount of multivalent cations required to precipitate DNA changes; tetravalent spermine is more efficient than the trivalent spermidine. The amount of multivalent cations required to resolubilize DNA varies by a factor of 4 between spermidine and spermine (Fig. 2d). We have plotted the DNA in solution (%) as a function of molecular ratio (±) (Fig. S15). We find the same charge-to-molar ratio for DNA precipitation and solubilization using these two analytical methods.

Towards a translocation of a condensing DNA

DNA condensation induced by multivalent cations has been intensively studied for many decades, motivated by the emergence of attractive interactions mediated by multivalent counterions condensing onto DNA. For example, the phase diagram was previously explained using an ion-bridging model based on short-range electrostatic attractions.[16,52] Other approaches based on ionic correlations were also developed at that time. DNA is one of the highly charged polyelectrolytes where translocation can be modulated by electrostatic potential interactions within the solid-state pore.[53] In addition, under an applied voltage, the electrostatic force exerted on the bare charged DNA drives its translocation through a pore. However, the electrophoretic motion of the counterions in the opposite direction also leads to the emergence of an opposed drag force.[54] The present experiments may serve as a basis from which electrostatic effects (charge reduction, inversion, or attractive interactions) can be progressively introduced by drastically reducing the concentration of NaCl. Probing the dynamics of a condensing chain at the single-chain level would help to understand the attractive interactions.

Conclusion

We demonstrate that, after solid-state membrane passivation, we mainly prevent interactions between DNA and the nanopore surface, and then control the entry and transport of the DNA as a function of the applied voltage. We demonstrate the DNA precipitation and resolubilization phenomena by plotting the evolution of event frequency of molecules in the supernatant as a function of polyamine concentration. The addition of spermidine or spermine leads to a decrease in event frequency due to the precipitation of DNA by electrostatic attractive interactions. Further addition of polycations leads to an increase in DNA in solution due to the resolubilization of DNA aggregates. At high salt concentration, the event frequency is not affected by the addition of polyamines, due to a suppression of DNA precipitation. Bulk and single-molecule experiments yield the same results, with the same threshold concentration of polyamines for precipitation and resolubilization phenomena.

Nanopore recording is a very suitable technique for studying DNA phase transitions as a function of the environment. Here, we change the solvent quality by adding multivalent cations, which can be considered as a poor solvent. Our experiments pave the way for investigating DNA collapse or DNA phase separation in the presence of other compaction agents, such as basic proteins imply in chromatin compaction.

Author contributions

Y. C. performed the experiments and data analysis. Y. C., B. C., L. B., and J. P. designed the figures. J. P. and E. R. wrote the first draft, and Y. C., S. B., L. B., and B. C. participated in editing the manuscript JP designed the experiments.

Conflicts of interest

There are no conflicts to declare.

Data availability

The data supporting this article have been included as part of the supplementary information (SI). Supplementary information is available. See DOI: https://doi.org/10.1039/d5sc05267j.

Acknowledgements

This work was supported by the French Research Agency, ANR JCJC "QuaBioNHy" grant, ANR-23-CE44-0013. The authors would like to thank the China Scholarship Council for PhD fellowship funding.

References

1 A. Estévez-Torres and D. Baigl, DNA Compaction: Fundamentals and Applications, *Soft Matter*, 2011, **7**(15), 6746–6756, DOI: 10.1039/C1SM05373F.
2 S. Liu, A. Athreya, Z. Lao and B. Zhang, From Nucleosomes to Compartments: Physicochemical Interactions Underlying Chromatin Organization, *Annu. Rev. Biophys.*, 2024, **53**(53), 221–245, DOI: 10.1146/annurev-biophys-030822-032650.
3 R. Villaseñor and T. Baubec, Regulatory Mechanisms Governing Chromatin Organization and Function, *Curr. Opin. Cell Biol.*, 2021, **70**, 10–17, DOI: 10.1016/j.ceb.2020.10.015.
4 P. Scaffidi and T. Misteli, Cancer Epigenetics From Disruption of Differentiation Programs to the Emergence of Cancer Stem Cells, *Cold Spring Harb. Symp. Quant. Biol.*, 2010, **75**, 251–258, DOI: 10.1101/sqb.2010.75.007.
5 Y. Y. Lenis, M. A. Elmetwally, J. G. Maldonado-Estrada and F. W. Bazer, Physiological Importance of Polyamines, *Zygote*, 2017, **25**(3), 244–255, DOI: 10.1017/S0967199417000120.
6 C. E. Holbert, M. T. Cullen, R. A. Casero and T. M. Stewart, Polyamines in Cancer: Integrating Organismal Metabolism and Antitumour Immunity, *Nat. Rev. Cancer*, 2022, **22**(8), 467–480, DOI: 10.1038/s41568-022-00473-2.
7 S. Vrijsen, M. Houdou, A. Cascalho, J. Eggermont and P. Vangheluwe, Polyamines in Parkinson's Disease: Balancing Between Neurotoxicity and Neuroprotection,

Annu. Rev. Biochem., 2023, **92**(92), 435–464, DOI: **10.1146/annurev-biochem-071322-021330**.

8 J. L. Sikorav, J. Pelta and F. Livolant, A Liquid Crystalline Phase in Spermidine-Condensed DNA, *Biophys. J.*, 1994, **67**(4), 1387–1392, DOI: **10.1016/S0006-3495(94)80640-X**.

9 E. Raspaud, J. Pelta, M. de Frutos and F. Livolant, Solubility and Charge Inversion of Complexes of DNA and Basic Proteins, *Phys. Rev. Lett.*, 2006, **97**(6), 068103, DOI: **10.1103/PhysRevLett.97.068103**.

10 G. S. Manning, The Molecular Theory of Polyelectrolyte Solutions with Applications to the Electrostatic Properties of Polynucleotides, *Q. Rev. Biophys.*, 1978, **11**(2), 179–246, DOI: **10.1017/S0033583500002031**.

11 V. A. Bloomfield, Condensation of DNA by Multivalent Cations: Considerations on Mechanism, *Biopolymers*, 1991, **31**(13), 1471–1481, DOI: **10.1002/bip.360311305**.

12 P. G. Arscott, A.-Z. Li and V. A. Bloomfield, Condensation of DNA by Trivalent Cations. 1. Effects of DNA Length and Topology on the Size and Shape of Condensed Particles, *Biopolymers*, 1990, **30**(5–6), 619–630, DOI: **10.1002/bip.360300514**.

13 L. C. Gosule and J. A. Schellman, Compact Form of DNA Induced by Spermidine, *Nature*, 1976, **259**(5541), 333–335, DOI: **10.1038/259333a0**.

14 J. Pelta, D. Durand, J. Doucet and F. Livolant, DNA Mesophases Induced by Spermidine: Structural Properties and Biological Implications, *Biophys. J.*, 1996, **71**(1), 48–63, DOI: **10.1016/S0006-3495(96)79232-9**.

15 J. Pelta, F. Livolant and J.-L. Sikorav, DNA Aggregation Induced by Polyamines and Cobalthexamine, *J. Biol. Chem.*, 1996, **271**(10), 5656–5662, DOI: **10.1074/jbc.271.10.5656**.

16 E. Raspaud, M. Olvera De La Cruz, J.-L. Sikorav and F. Livolant, Precipitation of DNA by Polyamines: A Polyelectrolyte Behavior, *Biophys. J.*, 1998, **74**(1), 381–393, DOI: **10.1016/S0006-3495(98)77795-1**.

17 I. M. Fujinami Tanimoto, J. Zhang, B. Cressiot, B. Le Pioufle, L. Bacri and J. Pelta, Dynamics of DNA Through Solid-State Nanopores Fabricated by Controlled Dielectric Breakdown, *Chem.–Asian J.*, 2022, **17**(24), e202200888, DOI: **10.1002/asia.202200888**.

18 C. Lu, A. Bonini, J. H. Viel and G. Maglia, Toward Single-Molecule Protein Sequencing Using Nanopores, *Nat. Biotechnol.*, 2025, **43**(3), 312–322, DOI: **10.1038/s41587-025-02587-y**.

19 L. Ratinho, N. Meyer, S. Greive, B. Cressiot and J. Pelta, Nanopore Sensing of Protein and Peptide Conformation for Point-of-Care Applications, *Nat. Commun.*, 2025, **16**(1), 3211, DOI: **10.1038/s41467-025-58509-8**.

20 L. Xu and M. Seki, Recent Advances in the Detection of Base Modifications Using the Nanopore Sequencer, *J. Hum. Genet.*, 2020, **65**(1), 25–33, DOI: **10.1038/s10038-019-0679-0**.

21 Y.-L. Ying, Z.-L. Hu, S. Zhang, Y. Qing, A. Fragasso, G. Maglia, A. Meller, H. Bayley, C. Dekker and Y.-T. Long, Nanopore-Based Technologies beyond DNA Sequencing, *Nat. Nanotechnol.*, 2022, **17**(11), 1136–1146, DOI: **10.1038/s41565-022-01193-2**.

22 C. Merstorf, O. Maciejak, J. Mathé, M. Pastoriza-Gallego, B. Thiebot, M.-J. Clément, J. Pelta, L. Auvray, P. A. Curmi and P. Savarin, Mapping the Conformational Stability of Maltose Binding Protein at the Residue Scale Using Nuclear Magnetic Resonance Hydrogen Exchange Experiments, *Biochemistry*, 2012, **51**(44), 8919–8930, DOI: **10.1021/bi3003605**.

23 G. Oukhaled, J. Mathé, A.-L. Biance, L. Bacri, J.-M. Betton, D. Lairez, J. Pelta and L. Auvray, Unfolding of Proteins and Long Transient Conformations Detected by Single Nanopore Recording, *Phys. Rev. Lett.*, 2007, **98**(15), 158101, DOI: **10.1103/PhysRevLett.98.158101**.

24 L. Payet, M. Martinho, M. Pastoriza-Gallego, J.-M. Betton, L. Auvray, J. Pelta and J. Mathé, Thermal Unfolding of Proteins Probed at the Single Molecule Level Using Nanopores, *Anal. Chem.*, 2012, **84**(9), 4071–4076, DOI: **10.1021/ac300129e**.

25 K. J. Freedman, S. R. Haq, J. B. Edel, P. Jemth and M. J. Kim, Single Molecule Unfolding and Stretching of Protein Domains inside a Solid-State Nanopore by Electric Field, *Sci. Rep.*, 2013, **3**(1), 1638, DOI: **10.1038/srep01638**.

26 D. Rodriguez-Larrea and H. Bayley, Multistep Protein Unfolding during Nanopore Translocation, *Nat. Nanotechnol.*, 2013, **8**(4), 288–295, DOI: **10.1038/nnano.2013.22**.

27 J. Nivala, D. B. Marks and M. Akeson, Unfoldase-Mediated Protein Translocation through an α-Hemolysin Nanopore, *Nat. Biotechnol.*, 2013, **31**(3), 247–250, DOI: **10.1038/nbt.2503**.

28 C. Merstorf, B. Cressiot, M. Pastoriza-Gallego, A. Oukhaled, J.-M. Betton, L. Auvray and J. Pelta, Wild Type, Mutant Protein Unfolding and Phase Transition Detected by Single-Nanopore Recording, *ACS Chem. Biol.*, 2012, **7**(4), 652–658, DOI: **10.1021/cb2004737**.

29 J. Li, Y. Wang, L. Wang, Y. Wang, Z. Zhang, S. Liu and L. Wang, Hofmeister Effect Matters in Nanopore Stoichiometry, *ACS Mater. Lett.*, 2025, **7**(7), 2476–2481, DOI: **10.1021/acsmaterialslett.5c00134**.

30 W. Chen, Y. Chen, Y. Wang, L. Chen, S. Zhou, D. Li, B. Yin, Z. Yang, L. Wang and H. Wang, Nanoscale Observation of Heparin-Mediated Self-Assembly of Chiral Tau Enantiomers, *Mater. Today Phys.*, 2024, **42**, 101370, DOI: **10.1016/j.mtphys.2024.101370**.

31 N. Giamblanco, D. Coglitore, T. Ma, P. E. Coulon, E. Balanzat, M. Bechelany, J.-M. Janot and S. Balme, Amyloid Fibril Analysis Using Single Nanopore, *Biophys. J.*, 2018, **114**(3), 181a, DOI: **10.1016/j.bpj.2017.11.1010**.

32 N. Martyushenko, W. Bell, D. Lamboll and U. F. Keyser, Nanopore Analysis of Amyloid Fibrils Formed by Lysozyme Aggregation, *Analyst*, 2015, **140**(14), 4882–4886, DOI: **10.1039/C5AN00530B**.

33 L. Zhan, T. Jin, J. Zhou, W. Xu, Y. Chen and R. Mezzenga, Fast Probing Amyloid Polymorphism *via* Nanopore Translocation, *Nano Lett.*, 2023, **23**(21), 9912–9919, DOI: **10.1021/acs.nanolett.3c02860**.

34 F. Piguet, H. Ouldali, F. Discala, M.-F. Breton, J. C. Behrends, J. Pelta and A. Oukhaled, High Temperature Extends the

Range of Size Discrimination of Nonionic Polymers by a Biological Nanopore, *Sci. Rep.*, 2016, **6**(1), 38675, DOI: 10.1038/srep38675.

35 M. Wanunu, J. Sutin, B. McNally, A. Chow and A. Meller, DNA Translocation Governed by Interactions with Solid-State Nanopores, *Biophys. J.*, 2008, **95**(10), 4716–4725.

36 M. Wanunu, W. Morrison, Y. Rabin, A. Y. Grosberg and A. Meller, Electrostatic Focusing of Unlabelled DNA into Nanoscale Pores Using a Salt Gradient, *Nat. Nanotechnol.*, 2010, **5**(2), 160–165, DOI: 10.1038/nnano.2009.379.

37 A. J. Storm, C. Storm, J. Chen, H. Zandbergen, J.-F. Joanny and C. Dekker, Fast DNA Translocation through a Solid-State Nanopore, *Nano Lett.*, 2005, **5**(7), 1193–1197, DOI: 10.1021/nl048030d.

38 I. M. Fujinami Tanimoto, J. Zhang, B. Cressiot, B. Le Pioufle, L. Bacri and J. Pelta, Dynamics of DNA Through Solid-state Nanopores Fabricated by Controlled Dielectric Breakdown, *Chem.–Asian J.*, 2022, **17**(24), e202200888, DOI: 10.1002/asia.202200888.

39 J. Li, M. Gershow, D. Stein, E. Brandin and J. A. Golovchenko, DNA Molecules and Configurations in a Solid-State Nanopore Microscope, *Nat. Mater.*, 2003, **2**(9), 611–615, DOI: 10.1038/nmat965.

40 C. Plesa, D. Verschueren, S. Pud, J. van der Torre, J. W. Ruitenberg, M. J. Witteveen, M. P. Jonsson, A. Y. Grosberg, Y. Rabin and C. Dekker, Direct Observation of DNA Knots Using a Solid-State Nanopore, *Nat. Nanotechnol.*, 2016, **11**(12), 1093–1097, DOI: 10.1038/nnano.2016.153.

41 D. Fologea, E. Brandin, J. Uplinger, D. Branton and J. Li, DNA Conformation and Base Number Simultaneously Determined in a Nanopore, *Electrophoresis*, 2007, **28**(18), 3186–3192, DOI: 10.1002/elps.200700047.

42 J. Feng, K. Liu, R. D. Bulushev, S. Khlybov, D. Dumcenco, A. Kis and A. Radenovic, Identification of Single Nucleotides in MoS2 Nanopores, *Nat. Nanotechnol.*, 2015, **10**(12), 1070–1076, DOI: 10.1038/nnano.2015.219.

43 Z. Wang, F. Qin, J. Wu, W. Ma, R. Li, T. Weng, B. Yin, L. Wang, D. Wang and L. Liang, Single-Molecule Recognition of Nucleolin and the Interactions with DNA/RNA G-Quadruplexes *via* Nanopore Decoding, *Chem. Eng. J.*, 2023, **473**, 145311.

44 M. Waugh, K. Briggs, D. Gunn, M. Gibeault, S. King, Q. Ingram, A. M. Jimenez, S. Berryman, D. Lomovtsev, L. Andrzejewski and V. Tabard-Cossa, Solid-State Nanopore Fabrication by Automated Controlled Breakdown, *Nat. Protoc.*, 2020, **15**(1), 122–143, DOI: 10.1038/s41596-019-0255-2.

45 I. Abrao-Nemeir, J. Bentin, N. Meyer, J.-M. Janot, J. Torrent, F. Picaud and S. Balme, Investigation of α-Synuclein and Amyloid-β(42)-E22Δ Oligomers Using SiN Nanopore Functionalized with L-Dopa, *Chem.–Asian J.*, 2022, **17**(20), e202200726, DOI: 10.1002/asia.202200726.

46 B. Cressiot, A. Oukhaled, G. Patriarche, M. Pastoriza-Gallego, J.-M. Betton, L. Auvray, M. Muthukumar, L. Bacri and J. Pelta, Protein Transport through a Narrow Solid-State Nanopore at High Voltage: Experiments and Theory, *ACS Nano*, 2012, **6**(7), 6236–6243, DOI: 10.1021/nn301672g.

47 L. Brun, M. Pastoriza-Gallego, G. Oukhaled, J. Mathé, L. Bacri, L. Auvray and J. Pelta, Dynamics of Polyelectrolyte Transport through a Protein Channel as a Function of Applied Voltage, *Phys. Rev. Lett.*, 2008, **100**(15), 158302, DOI: 10.1103/PhysRevLett.100.158302.

48 R. Erickson, I. Cohen, F. Messing, E. Nordberg, R. Siemann, J. Smith-Kintner, P. Stein, G. Drews, W. Gebert, F. Janata, P. Joos, A. Ladage, H. Nagel, H. Preissner and P. Söding, Charge Retention in Deep-Inelastic Electroproduction, *Phys. Rev. Lett.*, 1979, **42**(13), 822–825, DOI: 10.1103/PhysRevLett.42.822.

49 G. Gibrat, M. Pastoriza-Gallego, B. Thiebot, M.-F. Breton, L. Auvray and J. Pelta, Polyelectrolyte Entry and Transport through an Asymmetric α-Hemolysin Channel, *J. Phys. Chem. B*, 2008, **112**(47), 14687–14691, DOI: 10.1021/jp808088y.

50 M. Muthukumar, Theory of Capture Rate in Polymer Translocation, *J. Chem. Phys.*, 2010, **132**(19), 195101, DOI: 10.1063/1.3429882.

51 N. A. W. Bell, M. Muthukumar and U. F. Keyser, Translocation Frequency of Double-Stranded DNA through a Solid-State Nanopore, *Phys. Rev. E*, 2016, **93**(2), 022401, DOI: 10.1103/PhysRevE.93.022401.

52 M. O. De La Cruz, L. Belloni, M. Delsanti, J. P. Dalbiez, O. Spalla and M. Drifford, Precipitation of Highly Charged Polyelectrolyte Solutions in the Presence of Multivalent Salts, *J. Chem. Phys.*, 1995, **103**(13), 5781–5791, DOI: 10.1063/1.470459.

53 Y. Wang, M. Cheng, L. Wang, D. Zhou, S. He, L. Liang, F. Zhang, C. Liu, D. Wang and J. Yuan, Nanocrystalline Graphite Nanopores for DNA Sensing, *Carbon*, 2021, **176**, 271–278, DOI: 10.1016/j.carbon.2020.12.064.

54 S. Van Dorp, U. F. Keyser, N. H. Dekker, C. Dekker and S. G. Lemay, Origin of the Electrophoretic Force on DNA in Solid-State Nanopores, *Nat. Phys.*, 2009, **5**(5), 347–351.